Proc. 29th Int. Workshop on Vertex Detectors (VERTEX2020)
JPS Conf. Proc. **34**, 010017 (2021)
https://doi.org/10.7566/JPSCP.34.010017

A Study of Hit-time Reconstruction of Belle II Silicon Vertex Detector

Y. Uematsu[19], K. Adamczyk[22], H. Aihara[19], T. Aziz[12], S. Bacher[22], S. Bahinipati[8], G. Batignani[13,14], J. Baudot[6], P. K. Behera[9], S. Bettarini[13,14], T. Bilka[5], A. Bozek[22], F. Buchsteiner[2], G. Casarosa[13,14], Y. Q. Chen[4], L. Corona[13,14], T. Czank[18], S. B. Das[10], N. Dash[9], G. Dujany[6], F. Forti[13,14], M. Friedl[2], E. Ganiev[15,16], B. Gobbo[16], S. Halder[12], K. Hara[20,17], S. Hazra[12], T. Higuchi[18], C. Irmler[2], A. Ishikawa[20,17], H. B. Jeon[21], Y. Jin[16], C. Joo[18], M. Kaleta[22], A. B. Kaliyar[12], J. Kandra[5], K. H. Kang[21], P. Kapusta[22], P. Kodyš[5], T. Kohriki[20], M. Kumar[10], R. Kumar[11], P. Kvasnička[5], C. La Licata[18], K. Lalwani[10], S. C. Lee[21], Y. B. Li[3], J. Libby[9], S. N. Mayekar[12], G. B. Mohanty[12], T. Morii[18], K. R. Nakamura[20,17], Z. Natkaniec[22], Y. Onuki[19], W. Ostrowicz[22], A. Paladino[13,14], E. Paoloni[13,14], H. Park[21], G. Polat[7], K. K. Rao[12], I. Ripp-Baudot[6], G. Rizzo[13,14], N. Rout[9], D. Sahoo[12], C. Schwanda[2], J. Serrano[7], J. Suzuki[20], S. Tanaka[20,17], H. Tanigawa[19], R. Thalmeier[2], T. Tsuboyama[20,17], O. Verbycka[22], L. Vitale[15,16], K. Wan[19], J. Webb[1], J. Wiechczynski[14], H. Yin[2], L. Zani[7]

(Belle-II SVD Collaboration)

[1]*School of Physics, University of Melbourne, Melbourne, Victoria 3010, Australia*
[2]*Institute of High Energy Physics, Austrian Academy of Sciences, 1050 Vienna, Austria*
[3]*Peking University, Department of Technical Physics, Beijing 100871, China*
[4]*University of Science and Technology of China, Department of Modern Physics, Hefei 230026, China*
[5]*Faculty of Mathematics and Physics, Charles University, 121 16 Prague, Czech Republic*
[6]*IPHC, UMR 7178, Université de Strasbourg, CNRS, 67037 Strasbourg, France*
[7]*Aix Marseille Université, CNRS/IN2P3, CPPM, 13288 Marseille, France*
[8]*Indian Institute of Technology Bhubaneswar, Satya Nagar, India*
[9]*Indian Institute of Technology Madras, Chennai 600036, India*
[10]*Malaviya National Institute of Technology Jaipur, Jaipur 302017, India*
[11]*Punjab Agricultural University, Ludhiana 141004, India*
[12]*Tata Institute of Fundamental Research, Mumbai 400005, India*
[13]*Dipartimento di Fisica, Università di Pisa, I-56127 Pisa, Italy*
[14]*INFN Sezione di Pisa, I-56127 Pisa, Italy*
[15]*Dipartimento di Fisica, Università di Trieste, I-34127 Trieste, Italy*
[16]*INFN Sezione di Trieste, I-34127 Trieste, Italy*
[17]*The Graduate University for Advanced Studies (SOKENDAI), Hayama 240-0193, Japan*
[18]*Kavli Institute for the Physics and Mathematics of the Universe (WPI), University of Tokyo, Kashiwa 277-8583, Japan*
[19]*Department of Physics, University of Tokyo, Tokyo 113-0033, Japan*
[20]*High Energy Accelerator Research Organization (KEK), Tsukuba 305-0801, Japan*
[21]*Department of Physics, Kyungpook National University, Daegu 41566, Korea*
[22]*H. Niewodniczanski Institute of Nuclear Physics, Krakow 31-342, Poland*

E-mail: uematsu@hep.phys.s.u-tokyo.ac.jp

(Received December 10, 2020)

For stable operation of the Belle II Silicon Vertex Detector in the future high-luminosity operation of SuperKEKB, we plan to reduce readout data-samples per trigger and to apply hit-selection using hit-time. To realize this plan, we developed novel hit-time estimation methods, one of which achieves the resolution of 2.28 ± 0.04 ns evaluated in the current data acquisition mode. A study using Monte Carlo simulation also confirms that the hit-selection based on this hit-time improves track reconstruction performance.

KEYWORDS: Belle II, silicon tracker, timing resolution

1. Introduction

The Belle II experiment [1] started operation with the present vertex detector in the spring of 2019. The experiment aims to probe new physics beyond the Standard Model by analyzing a large number of final states, mainly from decays of $B\overline{B}$-pairs, in high-luminosity e^+e^- collisions at SuperKEKB (KEK, Japan) [2].

The vertex detector consists of the Silicon Vertex Detector (SVD) and the Pixel Detector (PXD). In particular, SVD includes four layers of Double-sided Silicon Strip Detectors (DSSDs), which provide two-dimensional hit position information for the track reconstruction. SVD is crucial for pointing at a region-of-interest limiting the PXD read-out volume (see Sect. 4.7.5 in Ref. 1), the track reconstruction of low-momentum charged particles, and the precise measurement of K_S decay vertices.

2. Future concerns and updates for stable SVD operation

During the first year of data taking, SVD has demonstrated very stable and excellent performance. One of the next operational challenges will be the large amount of beam-related background caused by the future high-luminosity operation of SuperKEKB. We will have a higher trigger rate of 30 kHz by design and a higher hit occupancy from this background. There are mainly two concerns for SVD operation under these conditions: various data bandwidths and track reconstruction performance.

2.1 Various data bandwidths

SVD data are read out at the reception of the Belle II global trigger. There are many steps for data readout, and hence various limiting bandwidths. In the high-luminosity operation, the higher trigger rate and the larger data-size of background hits will make the data-rate exceed those bandwidths, causing data loss. To avoid this data acquisition (DAQ) inefficiency, we need to reduce the data-size beforehand. Such reduction can be realized at the frontend ASIC, *APV25* [3]. APV25 processes data through FIFO at a sampling rate of 31.8 MHz and sends six successive ADC samples at the trigger arrival. Here, we can reduce the number of readout samples from six to three (3-sample-mode DAQ) keeping the same sampling rate. Note that if the trigger timing is precise enough, the effect on SVD performance stays small and under control, even though we have only three samples. Besides the data-size reduction per hit, we can gain more data reduction because the number of background hits decreases due to the narrower sampling time window.

2.2 Track reconstruction performance

Another concern is the track reconstruction: the more background hits in one event, the more difficult the track reconstruction is. A large number of background hits cause a much larger number of hit-combinations. Since it becomes more difficult to find correct tracks from a large number of these possible candidates, track reconstruction efficiency decreases, and fake-rate increases. We can improve this situation by rejecting efficiently the background hits in offline reconstruction. One solution

for this is to use hit-time information. Particles from the physics event come from a specific collision bunch-crossing, while the particles from beam-related backgrounds can come from any bunches. The hit-time tells which bunch-crossing creates the hits. Therefore, we can reject the background hits by applying cuts on the hit-time.

3. Novel hit-time estimation methods for future DAQ

To realize both 3-sample-mode DAQ and hit-selection based on hit-time, we need to establish hit-time estimation methods that work on hit data with only three ADC samples. Here, we developed two novel time estimation methods: *CoG3* and *ELS3* [4]. In CoG3, the hit-time estimator is the average of the acquired times of three ADC samples ($T = 0$ defined at the first sampling point) weighted by their ADC values, as shown in Eq. (1). In ELS3, we approximate the pulse shape with the impulse response of the CR-RC shaper and then fit the acquired three ADC samples. For this fitting, we can calculate the minimization analytically and hence the resulting fit parameters. Note that the two estimation methods yield quite different raw times before calibration (see Sect. 4.1). With three ADC samples a_0, a_1, a_2, sampling period of APV25 $\Delta t = 31$ ns, and CR-RC shaper time-constant for ELS3 $\tau = 55$ ns, the estimators can be written down as

$$T_{\mathrm{SVD;raw}}(\mathrm{CoG3}) = \frac{a_1 + 2a_2}{a_0 + a_1 + a_2} \cdot \Delta t, \tag{1}$$

$$T_{\mathrm{SVD;raw}}(\mathrm{ELS3}) = -\frac{2e^{-4\Delta t/\tau} + \frac{a_0 - e^{-2\Delta t/\tau} a_2}{2a_0 + e^{-\Delta t/\tau} a_1} \cdot e^{-2\Delta t/\tau}}{1 - e^{-4\Delta t/\tau} - \frac{a_0 - e^{-2\Delta t/\tau} a_2}{2a_0 + e^{-\Delta t/\tau} a_1} \cdot \left(2 + e^{-2\Delta t/\tau}\right)} \cdot \Delta t. \tag{2}$$

4. Performance of the novel hit-time estimation in the current DAQ

We applied the above methods on the data of *hadron* events [5] taken with the current DAQ, where we have six ADC samples per hit. To apply CoG3 or ELS3, we choose three successive ADC samples from the six. For sufficient information, these three samples need to include (a) the highest ADC value of the six to estimate the amplitude properly and (b) the rising edge of the waveform, which is steeper than the falling, to estimate the hit-time. To satisfy these requirements, we take two successive samples with the highest sum (a) and one sample before (b). Among the candidates, we confirm that this selection gives us the best hit-time resolution. Note that this selection is applied offline, while in a real online implementation, we should tune the latency to the trigger time as we cannot use the waveform information.

4.1 Calibration

Though the estimators derived from the above methods correlate to the true hit-time, they do not directly give us the true hit-time. To calibrate the hit-time estimators, we use the time of the corresponding bunch-crossing estimated offline by the outer detectors, called "EventT0" or t_0, which has a 0.65 ± 0.01 ns resolution. To compare with the hit-time estimation of SVD and EventT0, we shift the EventT0 to get synchronized to the SVD reference frame, called "synchronized EventT0" or t_0^{sync}. To extract the correlation, we reduce the effect of the background hits by using only the hits associated with the reconstructed track. The correlation plots for CoG3 and ELS3 are shown in Fig. 1. Calibration function shapes used in the fit to the correlations are found empirically:

$$\mathrm{CoG3} : T_{\mathrm{SVD}} = a + b \cdot T_{\mathrm{SVD;raw}} + c \cdot \left(T_{\mathrm{SVD;raw}}\right)^2 + d \cdot \left(T_{\mathrm{SVD;raw}}\right)^3, \tag{3}$$

$$\mathrm{ELS3} : T_{\mathrm{SVD}} = a + b \cdot T_{\mathrm{SVD;raw}} + \frac{c}{T_{\mathrm{SVD;raw}} - d}. \tag{4}$$

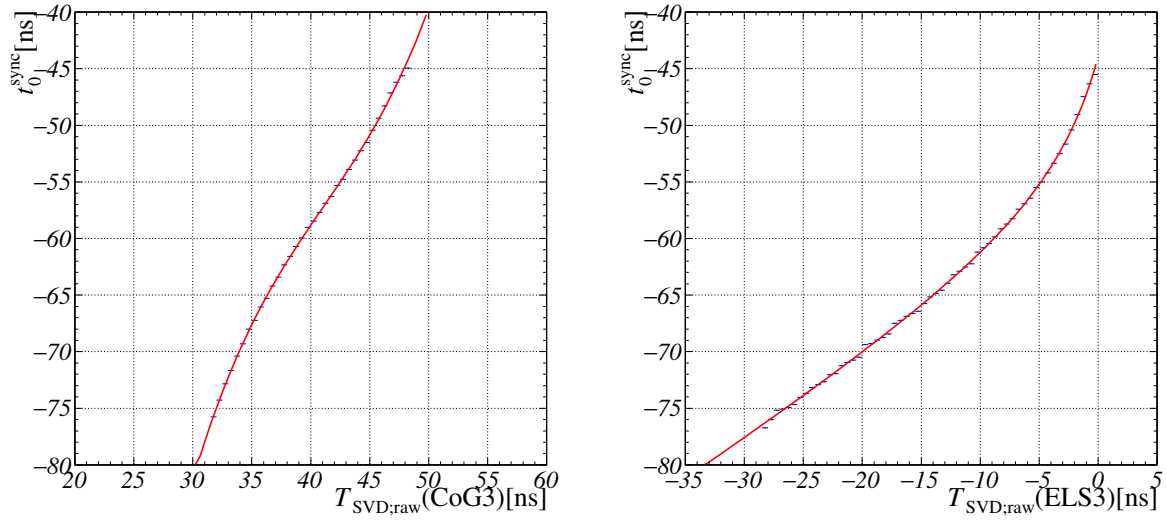

Fig. 1. Correlation plots for hit-time estimator in CoG3/ELS3 and $t_0^{\rm sync}$ in real data of hadron events are shown in left/right plots, respectively. Black points with dark-blue error bars show the averaged value of $t_0^{\rm sync}$ at each $T_{\rm SVD;raw}$ bin: vertical error for the uncertainty of the mean and horizontal error for the bin width. Red curves show the fitted functions.

4.2 Hit-time distribution and resolution

Since the instability of the calibration is confirmed to be small [6], we apply the above calibration to the same data sets. The calibrated hit-time distributions for signal and background are shown in Fig. 2. Both distributions show a clear separation between signal and background. The difference observed in the background hit-time distribution between CoG3 and ELS3 comes from the different calibration functions.

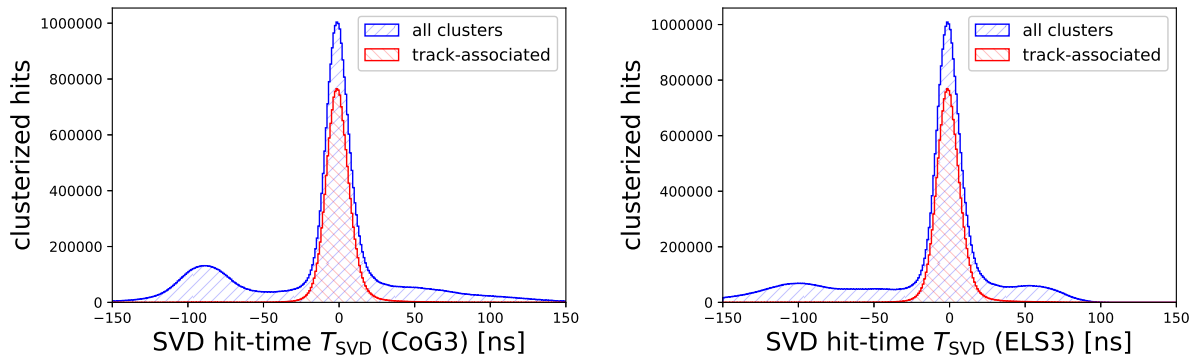

Fig. 2. Calibrated hit-time distributions derived by CoG3/ELS3 in real data of hadron events are shown in left/right plots, respectively. The red histogram is for the hits used in reconstructed tracks (i.e., signal hits), and the blue histogram is for all the hits, including both signal and background.

By subtracting $t_0^{\rm sync}$, we can remove trigger jitter from the hit-time. The distributions of this time residual are shown in Fig. 3. The signal peak gets sharper and shows better separation compared to

Fig. 2, before the subtraction. By subtracting the EventT0 resolution (see Sect. 4.1) from the width of the distribution [7], we can get the intrinsic hit-time resolution of 2.36 ± 0.04 ns/2.28 ± 0.04 ns for CoG3/ELS3. Due to this powerful hit-time resolution, we can observe a periodical structure every 12 ns in the background hit-time distribution, which corresponds to the bunch fill pattern.

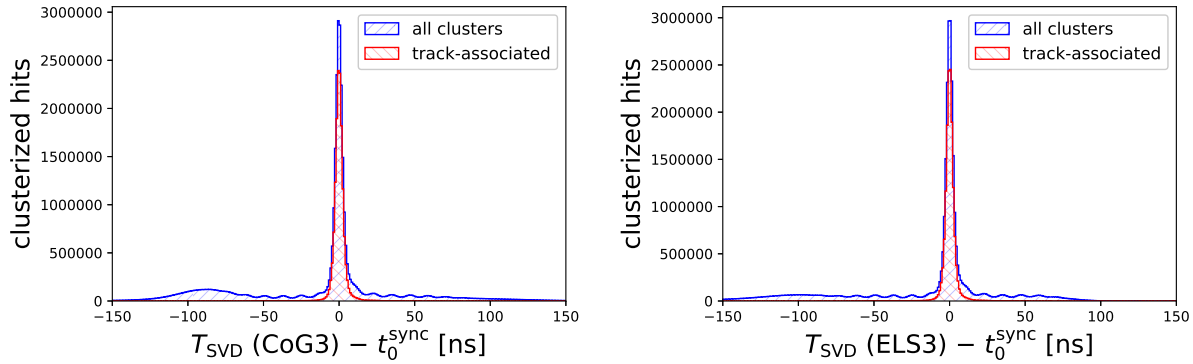

Fig. 3. Time residuals to t_0^{sync} derived by CoG3/ELS3 in real data of hadron events are shown in left/right plots, respectively. The red histogram is for the hits used in reconstructed tracks (i.e., signal hits), and the blue histogram is for all the hits, including both signal and background.

5. Performance of hit-selection using hit-time in simulation

We also studied the hit-time performance in Monte Carlo simulated samples, where we simulate the various amount of beam-related backgrounds. We simulate the current DAQ mode data and trace the same procedure as described in Sect. 4. The time residual of CoG3 is shown in Fig. 4. As in data, we can separate the signal peak from the background tail. Here we applied $[-35, +35]$ ns (width 70 ns) cut and achieved the signal hit efficiency of $99.55 \pm 0.02\%$ and background hit rejection of $80.89 \pm 0.06\%$. This selection improves SVD-standalone tracking, as shown in Fig. 5. We have a higher tracking efficiency and a lower tracking fake-rate. For example, even with 5% of background hit occupancy in the SVD innermost layer (Layer 3), we achieve 90% for the SVD-standalone tracking efficiency and suppress the fake-track rate to ~20%. These results are significantly improved compared to those without hit-selection: ~70% efficiency and ~60% fake-rate.

6. Conclusions

The novel hit-time estimation methods we developed show remarkable performance, achieving the hit-time resolution of around 2.3 ns in data taken in the 2019 autumn commissioning. Using this hit-time information for hit-selection, we could restore the SVD-standalone track-finding efficiency and suppress the fake-rate demonstrated in the Monte Carlo simulation, even with the existence of many background hits. These results are promising for future stable operation of SVD with higher luminosity, higher trigger rate, and more background hits.

Regarding the implementation of the 3-sample-mode DAQ, we plan to use this online only for the trigger where precision timing is prospected. In this way, we can minimize the effect on the SVD performance. This “3-mixed-6-mode” is already implemented in the DAQ system, and the test is ongoing in a cosmic-ray run. Also, the 3-sample time algorithms are already available in analysis software and used to analyze the cosmic-ray data. For the hit-selection based on the hit-time, a more

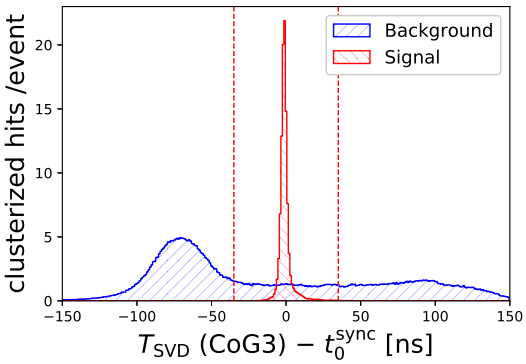

Fig. 4. The time residual derived by CoG3 in MC simulation is shown. The red histogram is for the signal, and the blue histogram is for the background. The events with hit-time between the two red vertical dashed-lines are selected for evaluation of the track-finding efficiency and fake-track rate.

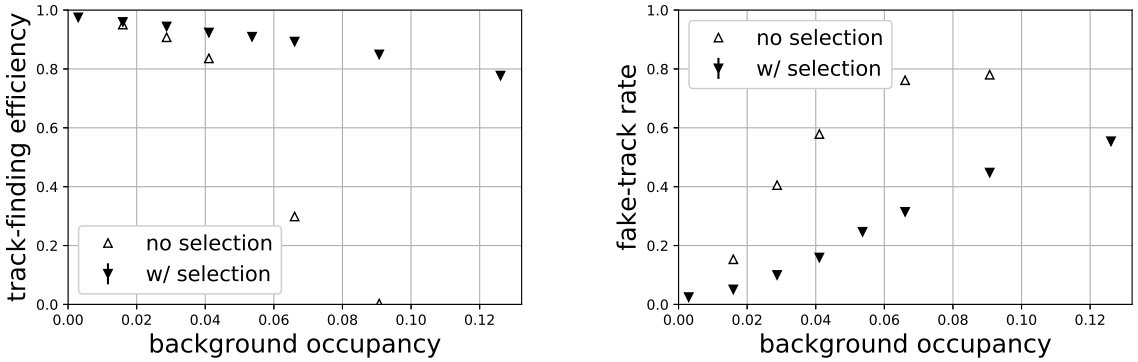

Fig. 5. The relation between SVD-standalone track-finding efficiency/fake-track rate and background occupancy in MC simulation are shown in left/right plots, respectively. The white triangles show the results without the hit-time selection, and the black inverse triangles show the results with the hit-time selection. Background occupancy is the average of the sensor-wide strip occupancies in Layer-3 sensors. In the high-luminosity operation, this occupancy will reach 3–5% though estimated with large uncertainty.

detailed study is ongoing.

Acknowledgments

This project has received funding from the European Union's Horizon 2020 research and innovation programme under the Marie Sklodowska-Curie grant agreements No 644294 and 822070. This work is supported by MEXT, WPI, and JSPS (Japan); ARC (Australia); BMWFW (Austria); MSMT (Czechia); CNRS/IN2P3 (France); AIDA-2020 (Germany); DAE and DST (India); INFN (Italy); NRF-2016K1A3A7A09005605 and RSRI (Korea); and MNiSW (Poland).

References

[1] T. Abe et al.; Belle II Technical Design Report (2010). arXiv:1011.0352.
[2] Y. Ohnishi et al.; Prog. Theor. Exp. Phys. **2013**, 03A011 (2013).
[3] M. J. French et al.; Nucl. Instrum. Methods Phys. Res., Sect. A **466**, 359 (2001).

[4] CoG for “Center of Gravity”, ELS for “Exponential Least-Squares”.
[5] The events with more than three good tracks and not like Bhabha scattering.
[6] The difference of the calibration functions in the fit region is less than 2 ns for 36 different data sets from 13 days of data-taking.
[7] The width is derived from the standard deviation of fitted double-Gaussian, 2.44 ± 0.04 ns/2.37 ± 0.03 ns for CoG3/ELS3.